**Colloid & Polymer Science** Colloid Polym Sci 272:447–455 (1994)

# Dynamic surface tension behavior of aqueous solutions of *N*-dodecyl-*N*,*N* dimethyl aminobetaine chlorohydrate

A. Pinazo,[1]) C.-H. Chang, and E. I. Franses

School of Chemical Engineering, Purdue University, West Lafayette, USA

*Abstract*: The adsorption behavior of *N*-dodecyl-*N*,*N* dimethyl aminobetaine chlorohydrate (DDAB · HCl) at the air/aqueous interface was studied for solutions in pure water and phosphate buffer (pH = 7.4). The equilibrium surface tension versus concentration curves were used to estimate the equilibrium adsorption parameters and CMCs. The buffer solution has a lower CMC and shows higher surface activity below the CMC than the pure water solution. Data and calculations of the dynamic tension behavior at constant-area conditions showed that the adsorption processes of DDAB · HCl solutions are about 10 to 300 times slower than those predicted by a diffusion-controlled model. A mixed kinetics adsorption model with a modified Langmuir–Hinshelwood kinetic equation, which considers an activation energy barrier for adsorption, was applied to find the kinetic adsorption parameters. The dynamic tension behavior at pulsating-area conditions with large amplitude was also examined for frequencies up to 90 cycles/min. The tension amplitude responses depended strongly on the concentration and frequency. Comparisons of diffusion-controlled model predictions and pulsating area tension data confirmed the need to use a mixed kinetics model. The latter model can improve the fit over the diffusion-controlled model, but it does not quantitatively match the observed tensions.

*Key words*: Dynamic surface tension – dynamic adsorption – pulsating bubble surfactometry – adsorption/diffusion-controlled – adsorption/mixed kinetics

## Introduction

*N*-*n*-alkylbetaines are amphoteric surfactants which are chemically stable but easily biodegradable, are good foaming agents, and are usually soluble in salt, acidic, and basic solutions [1]. Their low toxicity and irritancy have made them viable in many commercial applications in cosmetics, detergents, toiletries, and textile processing [2, 3]. Their dynamic adsorption behavior has received little attention, despite its importance in foaming and sudsing, which affect the efficacy and consumer acceptance of detergent products.

This paper describes the dynamic tension behavior of *N*-dodecyl-*N*,*N* dimethyl aminobetaine chlorohydrate (DDAB · HCl). For the bromide salt of this material, previous authors have reported the equilibrium tension behavior [4]. For other betaines, dynamic tension data have been reported [5]. Here, we report dynamic tensions of aqueous DDAB · HCl in water or in buffer solutions under either constant area or pulsating area conditions. The pH chosen (7.4) corresponds to textile processing conditions [6, 7]. The data are compared to models previously reported [8–10] and show that the tension drops more slowly than

[1]) Instituto de Technologia Quimica y Textil (C.S.I.C.), 18–26, Barcelona, Spain

predicted by the diffusion controlled model for a single surfactant, indicating slow adsorption/desorption processes.

## Materials and methods

The surfactant used was produced from commercial DDAB (from Tenneco España S.A.) as follows. DDAB was first purified by continuous extraction with anhydrous ethanol. After the product was dissolved (26% w/v) in 1 N HCl in methanol solution, diethyl ether was added until the appearance of a white solid. The mixture was allowed to crystallize at 4 °C for 24 h. The crystalline white solid (DDAB · HCl) was filtered and dried under vacuum.

The product purity ($MW = 308$ dalton) was examined by thin-layer chromatography (TLC), two-phase mixed indicator method [11], elemental analysis, IR spectroscopy, and $^1$H-NMR. The TLC analysis showed only one positive spot to the Dragendorf reaction [12]. Titration of 1 mM aqueous solution indicated a purity of 99%. Elemental analysis results were consistent with theoretical values:

| | C (%) | H (%) | N (%) |
|---|---|---|---|
| calculated | 62.45 | 11.05 | 4.55 |
| measured | 62.49 | 11.05 | 4.36 |

The infrared absorption spectrum of the surfactant prepared in a KBr pellet showed the expected carbonyl band at 1630 cm$^{-1}$. The $^1$H-NMR spectrum of DDAB · HCl in $D_2O$ showed the following chemical shifts. At 0.9 ppm (relative to TMS), there was a triplet corresponding to methyl protons ($CH_3$–$(CH_2)_{10}$). In the interval from 1.2 to 1.4 ppm, there was a straight chain methylene group multiplet ($CH_3$–$(CH_2)_{10}$–$CH_2N$). The shift at 3.4 ppm was a multiplet due to methyl groups anchored to the ammonium ($CH_2$–$N(CH_3)_2$–$CH_2$). Based on the results of all the analyses, we concluded that the purity of DDAB · HCl was higher than 99 wt%. Although this may be inadequate for absolute surface chemical purity [13], no further purification procedures were used.

Ultrapure water (distilled and then passed through a Millipore four-stage system) was used for preparing all samples. Buffer solutions at pH = 7.4 were prepared by using

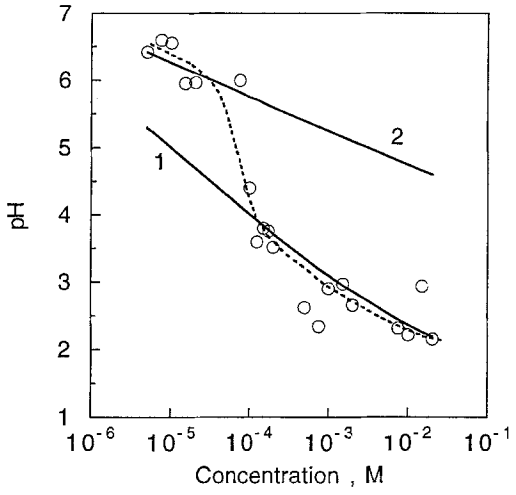


Fig. 1. Values of pH of aqueous solutions of DDAB · HCl below and above the CMC ( ~ $1.8 \cdot 10^{-4}$ M; see Fig. 2). For comparison, the predicted pH lines for nonmicellar betaine of pKa = 2.5 (curve 1) and 7.5 (curve 2) are also shown; $T = 25 \pm 1$ °C

$Na_2HPO_4 \cdot 12H_2O$ and $NaH_2PO_4 \cdot H_2O$ (obtained from Sigma Chemical Company) at a total concentration of 0.125 M. Figure 1 shows the measured pH values as a function of the surfactant concentration. For concentrations higher than $10^{-4}$ M, the measured pH values agree with the theoretical values found by using a pKa value of 2.5 reported for a similar molecule [14]. For concentrations lower than $10^{-4}$ M, the measured pH values are unexpectedly higher than those derived from a pKa of 2.5, and, in fact, would better fit an apparent pKa of 7.5. No explanation of the discrepancy is available.

Equilibrium surface tensions were measured with a platinum Wilhelmy plate tensiometer (Model K8, from Krüss), a spinning bubble tensiometer (Model 500, from the University of Texas), or a pulsating bubble surfactometer (PBS) (Electronetics Corporation, Amherst, New York). Dynamic tensions were measured with the pulsating bubble surfactometer (PBS) for constant-area and pulsating-area conditions. In the PBS measurements, the samples were loaded into a sample chamber, and a bubble with a radius of 0.4 mm was created. The temperature was controlled at 25 ± 1 °C by using a water bath. The pressure difference across the bubble was measured continually (about every 50 ms) after the bubble was formed (i.e., after the new air/liquid

interface was created). The surface tensions were calculated via the Laplace–Young equation through a preinstalled microprocessor in the instrument. The data were transferred to a Northgate 486 personal computer through an RS-232 interface. The bubble could be pulsated at rates of 1 to 100 cycles/min from a minimum radius of 0.40 mm to a maximum radius of 0.55 mm (area ratio 1.89). The dynamic tension response under pulsating-area conditions provides additional dynamic adsorption information [15].

## Results and discussion

### *Equilibrium surface tensions and adsorption parameters*

Tension measurements with the PBS method for various concentrations are shown in Fig. 2. Tensions for the buffer solutions below the CMC are generally lower than those for aqueous solutions. Its apparent CMC is also lower by 60%, apparently because of reduced intermolecular electrostatic effects at the higher ionic strength. The tension-concentration-based CMC of the aqueous solution was also measured with the spinning bubble tensiometry and was found close to the other value ($2.7 \pm 0.5 \times 10^{-4}$ vs. $1.8 \pm 0.2 \times 10^{-4}$ M). The CMC in buffer was tested with the Wilhelmy plate method and differed little from the PBS based value ($9 \pm 1 \times 10^{-5}$ vs. $7 \pm 1.0 \times 10^{-5}$ M). The discrepancies are probably due to the difficulties in establishing equilibrium surface tensions after long times, during which tensions can be affected by impurities. The lack of precision has little effect on the predicted dynamic tensions.

The data below the CMC were fit to the classical Szyszkowsky equation, which results from combining the Langmuir adsorption isotherm with the Gibbs adsorption isotherm:

$$\gamma = \gamma_0 - nRT\Gamma_m \ln(1 + K_L c)$$
$$= \gamma_0 + nRT\Gamma_m \ln(1 - \Gamma/\Gamma_m)\,, \qquad (1)$$

where $\gamma$ is the surface tension of the aqueous surfactant solution of concentration $c$, $\gamma_0$ is the surface tension of solvent (water), $R$ is the gas constant, $T$ is the absolute temperature, $\Gamma_m$ is the maximum surface concentration in the Langmuir

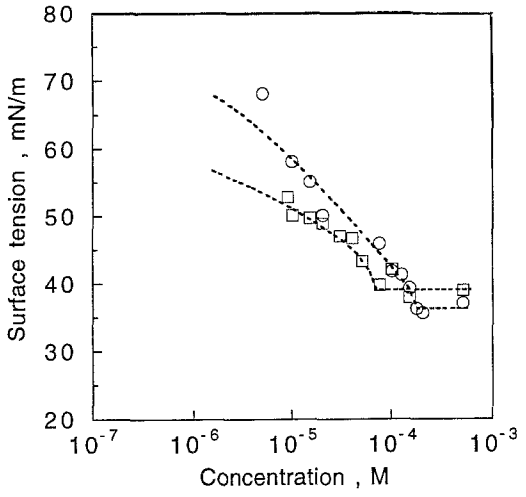


Fig. 2. Equilibrium surface tensions of aqueous DDAB · HCl solutions in pure water (○) and 0.125 M phosphate buffer (□, pH = 7.4); $T = 25 \pm 1$ °C

Table 1. CMCs and equilibrium adsorption parameters for DDAB–HCl from the PBS data of Fig. 2 (25 °C)

| Medium[a]) | CMC (M) | $\Gamma_m \cdot 10^6$ (mol · m$^{-2}$) | $K_L$ (m$^3$ · mol$^{-1}$) |
|---|---|---|---|
| *w* ($n = 3$)[b]) | $1.8 \pm 0.2 \cdot 10^{-4}$ | $1.0 \pm 0.1$ | $5.6 \pm 2.0 \cdot 10^2$ |
| *b*($n = 1$) | $7.0 \pm 1.0 \cdot 10^{-5}$ | $1.4 \pm 0.2$ | $4.1 \pm 3.9 \cdot 10^4$ |

[a]) *w*: water solution, *b*: buffer solution
[b]) see text for explanation of the value of $n$

adsorption model, and $K_L$ is the equilibrium adsorption constant. The parameter $n$ is the number of effective dissociated species per molecule for no added salt, or $n = 1$ for high concentration of electrolyte [16]. For our amphoteric surfactant, the dissociation below must be taken into account:

$$\text{DDAB} \cdot \text{HCl} \rightleftharpoons \text{DDAB}^{\pm} + \text{H}^+ + \text{Cl}^-\,. \qquad (2)$$

Hence, one has to use $n = 3$ here, analogously to 1:1 ionic surfactants which have $n = 2$ [16]. The best fit parameters ($\Gamma_m$ and $K_L$) in Eq. (1) were obtained with the Dow Chemical Simusolv software [17] and are listed in Table 1. The calculated surface tensions with the best fit parameters compare fairly well to the data.

The surfactant has a slightly larger apparent $\Gamma_m$ value in the buffer solution than in pure water. This can be accounted for by the expectation that electrostatic repulsions in the adsorbed monolayer

are reduced by the ionic strength effect. The equilibrium adsorption constant $K_L$, which is a measure of the surface activity [16], or the ability of the surfactant to reduce the surface tension at a given concentration, is a lot higher in the buffer solution than in pure water. Hence, the surfactant is much more surface active in the buffer (amphoteric form) than in water (partially cationic form). The estimates of $\Gamma_m$ and $K_L$ are approximate. Equation (1) is not expected to fit the data well, because the Langmuir isotherm assumptions (noninteracting point molecules on a lattice, and ultrapure surfactant) are hardly satisfied. Nonetheless, these values provide a good basis for calculating $\gamma(t)$ from the adsorbed density $\Gamma(t)$ (surface equation of state) and for calculating the expected dynamic tensions at the diffusion-controlled, or local equilibrium limit. More involved models would improve the accuracy of such calculations somewhat, but can hardly be justified with the present data.

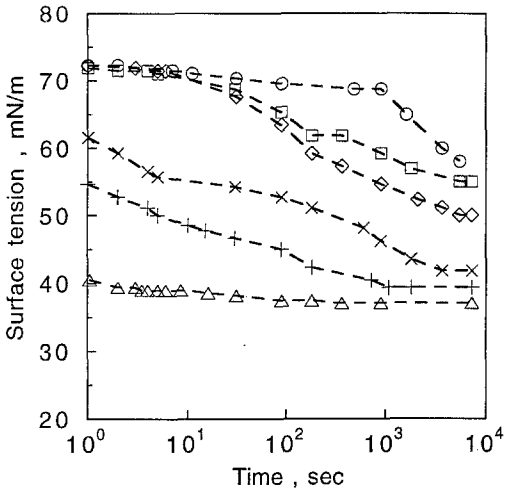


Fig. 3. Dynamic surface tensions of aqueous DDAB · HCl (at 25 ± 1°C) at constant-area conditions and concentrations of $1.0 \cdot 10^{-5}$ M (○), $1.5 \cdot 10^{-5}$ M (□), $2.0 \cdot 10^{-5}$ M (◇), $1.0 \cdot 10^{-4}$ M (×), $1.5 \cdot 10^{-4}$ M (+), and $5.0 \cdot 10^{-4}$ M (△)

*Dynamic surface tensions at constant-area conditions*

The dynamic surface tensions of the surfactant in water and buffer are plotted in Figs. 3 and 4. In each system, the first measurement was taken at about 1 s after the air/liquid interface was created. Most solutions (except at $5 \cdot 10^{-4}$ M) took much longer to equilibrate, $10^3$–$10^4$ s. The micellar solution ($5 \cdot 10^{-4}$ M) in water equilibrated in about 1 s, and in buffer in about 100 s. For $c_0 = 1.5 \cdot 10^{-4}$ M in the buffer solution, which is above the CMC, equilibration is slower than in the water solution, which is below the CMC.

To interpret the data quantitatively, we have calculated the times it took for adsorption to reach 10%, 50%, and 95% of its equilibrium value $\Gamma_e$, which was determined from the equilibrium data and Eq. (1). In Table 2, we also show the times predicted for premicellar solutions via a diffusion-controlled model, as detailed in ref. [8]. In this model, we use $D = 5 \cdot 10^{-10}$ m$^2$ s$^{-1}$ as a typical reasonable value for monomers, and we used a diffusion length $l$ much larger than the characteristic length for adsorption. The model is strictly valid for a one-component system, without allowing for possible impurities [8]. For low concentrations in water ($1 \cdot 10^{-5}$–$2 \cdot 10^{-5}$ M), the calculated diffusion timescales are 10 to 300 times

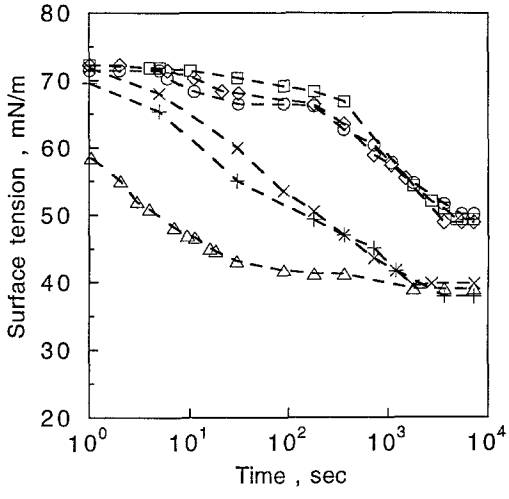


Fig. 4. Same as Fig. 3, but for solutions in phosphate buffer: $1.0 \cdot 10^{-5}$ M (○), $1.5 \cdot 10^{-5}$ M (□), $2.0 \cdot 10^{-5}$ M (◇), $7.5 \cdot 10^{-5}$ M (×), $1.5 \cdot 10^{-4}$ M (+), and $5.0 \cdot 10^{-4}$ M (△)

smaller than the measured ones, indicating that the process is adsorption-rate-limited or mixed-kinetic-controlled (or reflecting possible impurity effects, which cannot be quantified). At the highest concentration ($5 \cdot 10^{-4}$ M) which is higher than the CMC, the solution equilibrates faster than can be measured by the PBS instrument. Moreover, the predicted timescales are of

Table 2. Comparison of adsorption timescales ($t_{exp}$) to those ($t_L^*$) calculated from the diffusion-controlled model

| Solution concentration (M) | for 0.10 $\theta_e$ $t_{exp}$ (sec) | $t_L^*$ | for 0.50 $\theta_e$ $t_{exp}$ (sec) | $t_L^*$ | for 0.95 $\theta_e$ $t_{exp}$ (sec) | $t_L^*$ |
|---|---|---|---|---|---|---|
| $1.0 \cdot 10^{-5}$ *w***) | 8.7 | 0.11 | 1100 | 3.3 | 5000 | 74 |
| $1.0 \cdot 10^{-5}$ *b* | 1.0 | 0.31 | 6.0 | 7.6 | 550 | 29 |
| $1.5 \cdot 10^{-5}$ *w* | 4.0 | 0.055 | 57 | 1.5 | 2000 | 23 |
| $1.9 \cdot 10^{-5}$ *b* | 10 | 0.14 | 90 | 3.4 | 1000 | 13 |
| $2.0 \cdot 10^{-5}$ *w* | 2.0 | 0.032 | 11 | 0.89 | 800 | 10 |
| $2.0 \cdot 10^{-5}$ *b* | 2.0 | 0.076 | 12 | 1.9 | 610 | 7 |
| $5.0 \cdot 10^{-4}$ *w* | < 2.0 | 0.00006 | < 1.0 | 0.0015***) | < 1.0 | 0.0057 |
| $5.0 \cdot 10^{-4}$ *b* | < 1.0 | 0.00012 | < 1.0 | 0.0031 | < 1.0 | 0.011 |

**) *w*: water solution: *b*: buffer solution
***) the number was obtained without considering micellization

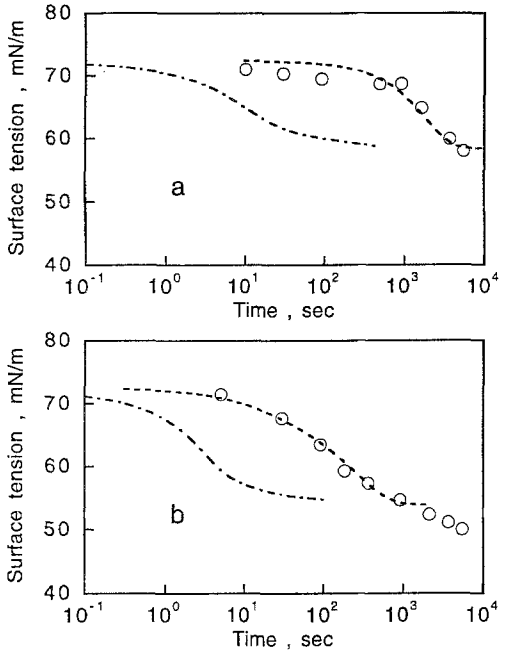


Fig. 5. Comparison of certain data of Fig. 3 to predictions of the diffusion-controlled model (·····) and the best-fit values of the mixed kinetics model (---) a) $1.0 \cdot 10^{-5}$ M, $k_L^a = 8.9 \cdot 10^{-8}\,\mathrm{m \cdot s^{-1}}$ and $B = 0$; b) $2.0 \cdot 10^{-5}$ M, $k_L^a = 3.6 \cdot 10^{-6}\,\mathrm{m\,s^{-1}}$ and $B = 3$

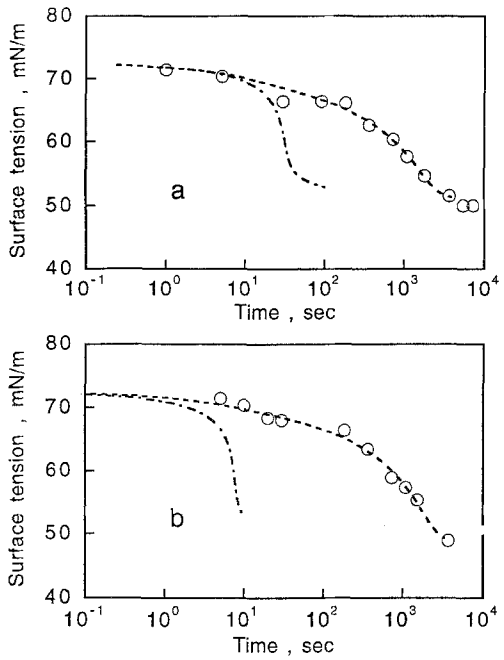


Fig. 6. Same as Fig. 5, but for solutions in phosphate buffer; a) $1.0 \cdot 10^{-5}$ M, $k_L^a = 2.0 \cdot 10^{-3}\,\mathrm{m \cdot s^{-1}}$ and $B = 9$; b) $2.0 \cdot 10^{-5}$ M, $k_L^a = 1.5 \cdot 10^{-4}\,\mathrm{m\,s^{-1}}$ and $B = 7$

the order of milliseconds. For the lowest concentration in buffer ($1 \cdot 10^{-5}$ M) and for $\Gamma/\Gamma_e = 0.1$ and 0.50, the process is close to being diffusion-controlled. At larger times at this concentration and for all higher concentrations, the process slows down compared to diffusion-controlled predictions, indicating that the adsorption/desorption is impeded by some kind of barrier at the surface. In Figs. 5 and 6, we show full comparisons between the data, the diffusion-controlled model, and the mixed kinetics model with the modified Langmuir–Hinshelwood

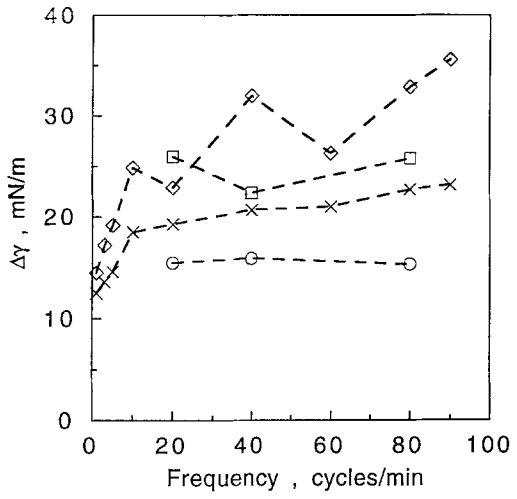


Fig. 7. Dynamic tension amplitudes ($\Delta\gamma = \gamma_{max} - \gamma_{min}$) for aqueous DDAB·HCl $1.0 \cdot 10^{-5}$ M (○), $2.0 \cdot 10^{-5}$ M (□), $1.0 \cdot 10^{-4}$ M (◇) and $2.0 \cdot 10^{-4}$ M (×) at various pulsating frequencies. The corresponding tension minima are shown in Table 3

kinetic equation [9],

$$\frac{d\Gamma}{dt} = k_L^a c(0, t)\left(1 - \frac{\Gamma}{\Gamma_m}\right)\exp\left(-B\frac{\Gamma}{\Gamma_m}\right) - k_L^d \Gamma \exp\left(-B\frac{\Gamma}{\Gamma_m}\right). \quad (3)$$

The parameters $k_L^a$ and $B$ are determined at each concentration by the best fit of the data to the model. The fits are fairly good. No single set of values of parameters can fit all concentrations, because apparently the adsorption rate parameters depend on surface coverage and solution ionic strength [9]. Not surprisingly, the $B$ parameters were found to be positive, indicating repulsive interactions. The adsorption rate parameters $k_L^a$ were found to be higher with the buffer, indicating decreasing repulsions because of screening of electrostatic interactions. These results are consistent with the inferences of the previous studies for sodium dodecylsulfate (SDS) and AOT surfactants [9]. This suggests the possibility that there is an activation energy barrier for the adsorption process of DDAB, which may be caused by the interactions between the surfactant molecules in the subsurface and the charged monolayer at the interface [9].

### *Dynamic surface tensions at pulsating-area conditions*

The dynamic tension behavior of DDAB·HCl was studied by the PBS method under pulsating-area conditions. For each solution, pulsation started after the equilibrium surface tension was attained. Hence, the initial condition for each pulsating experiment is the surface concentration at equilibrium with the bulk solution concentration. The tension amplitude responses $\Delta\gamma$ are plotted in Figs. 7 and 8. Results for the third cycle are shown for frequencies lower than 10 cycles/min. Otherwise, results for the 10th cycle are shown. The tension minima $\gamma_{min}$ at various conditions are listed in Table 3. For certain concentrations, only a limited number of frequencies were tested. The

Table 3. Tension minima $\gamma_{min}$ ($mN \cdot m^{-1}$) measured by the PBS method for DDAB·HCl solutions at different pulsating rates

| Concentration M | Pulsating rate, cycles per minute | | | | | | | | | |
|---|---|---|---|---|---|---|---|---|---|---|
| | 0*) | 1 | 3 | 5 | 10 | 20 | 40 | 60 | 80 | 90 |
| $1.0 \cdot 10^{-5}$ w**) | 58.1 | –***) | – | – | – | 55.1 | 54.7 | – | 55.8 | – |
| $2.0 \cdot 10^{-5}$ w | 50.1 | – | – | – | – | 44.0 | 45.1 | – | 44.7 | – |
| $1.0 \cdot 10^{-4}$ w | 41.9 | 37.0 | 35.6 | 34.3 | 32.2 | 31.7 | 27.1 | 32.1 | 27.9 | 26.8 |
| $2.0 \cdot 10^{-4}$ w | 32.9 | 26.3 | 27.4 | 26.0 | 26.0 | 26.4 | 24.8 | 24.9 | 25.7 | 25.2 |
| $1.0 \cdot 10^{-5}$ b**) | 52.4 | – | – | – | – | 50.5 | 50.5 | – | 51.6 | – |
| $2.0 \cdot 10^{-5}$ b | 48.9 | 48.4 | 46.3 | 44.9 | 44.0 | 43.6 | 43.4 | 43.6 | 44.0 | 43.2 |
| $1.0 \cdot 10^{-4}$ b | 42.1 | 39.5 | 36.2 | 34.7 | 32.7 | 31.2 | 30.2 | 31.7 | 32.1 | – |
| $5.0 \cdot 10^{-4}$ b | 39.0 | 35.9 | – | 36.8 | 33.9 | 33.7 | 31.7 | – | – | – |
| $2.0 \cdot 10^{-3}$ b | 35.9 | 35.1 | 35.5 | 35.0 | 34.3 | 33.9 | 33.7 | 33.7 | 33.7 | 33.3 |

*) Equilibrium tension for each solution
**) w: water; b: buffer
***) Data are not available

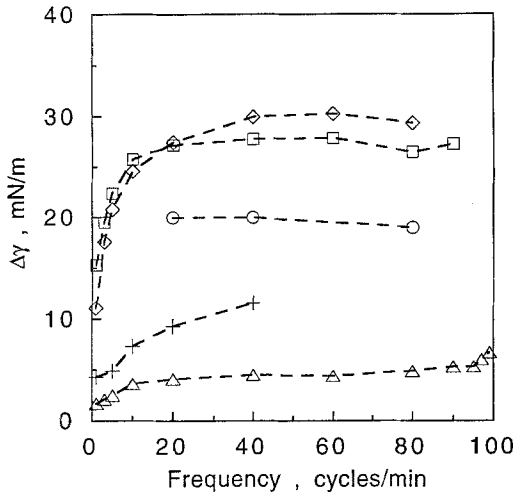


Fig. 8. Dynamic tension amplitudes at various pulating frequencies for $1.0 \cdot 10^{-5}$ M (○), $2.0 \cdot 10^{-5}$ M (□), $1.0 \cdot 10^{-4}$ M (◇), $5.0 \cdot 10^{-4}$ M ( + ), and $2.0 \cdot 10^{-3}$ M (△) DDAB·HCl in phosphate buffer. The tension minima are shown in Table 3

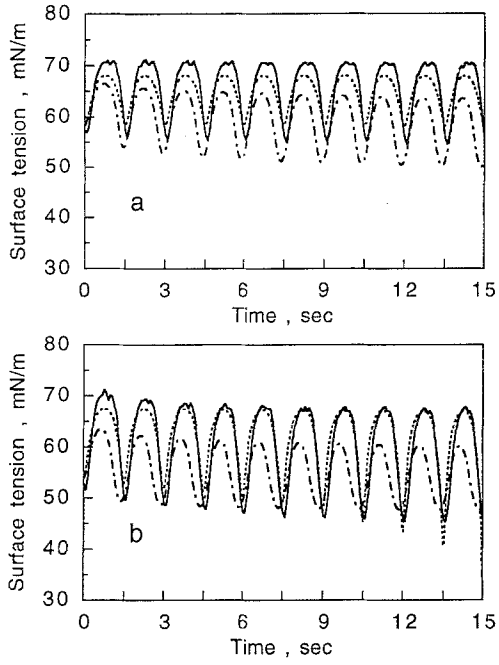


Fig. 9. Dynamic tension data (full lines) at pulsating-area conditions for aqueous DDAB·HCl, $1.0 \cdot 10^{-5}$ M a) and $2.0 \cdot 10^{-5}$ M b), 25 °C, at 40 cycles per minute. For comparison, lines are shown for the diffusion-controlled model (—·—) and the mixed kinetics adsorption model ( · · · )

amplitude $\Delta\gamma$ first increases with concentration and then decreases (Fig. 7). This behavior has been predicted from an adsorption model developed for pulsating area experiments [10]. For the extremely low concentrations, the surface coverage is relatively small during the pulsating stage, resulting in small $\Delta\gamma$. For the highest concentrations, the adsorption timescale is smaller than the oscillation period, resulting in smaller surface coverage variations and smaller tension variations. It appears that the optimal concentration for this system is around $1 \cdot 10^{-4}$ M. For frequencies up to 90 cycles/min, $\Delta\gamma$ increases with frequency for $1 \cdot 10^{-4}$ M and $2 \cdot 10^{-4}$ M solutions. For $1 \cdot 10^{-5}$ M and $2 \cdot 10^{-5}$ M solutions, $\Delta\gamma$ is almost constant or reaches a plateau for frequencies higher than 20 cycles/min. For the surfactant in buffer, the tension amplitudes (Fig. 8) are qualitatively similar to those in water solutions. The optimal concentration for maximum $\Delta\gamma$ is also about $1 \cdot 10^{-4}$ M. In Table 3, the listed minimum surface tensions obtained at different frequencies are always lower than the equilibrium surface tension. In the water solutions, the minimum tensions $\gamma_{min}$ always decrease as the concentration increases. But in the buffer solutions, the $\gamma_{min}$ first decreases as the concentration increases and then increases with concentration for the concentration higher than $1 \cdot 10^{-4}$ M.

With the kinetic adsorption parameters obtained from constant-area adsorption experiments, certain comparisons for the mixed kinetics model predictions and the experimental results are shown in Fig. 9 for surfactant in water. Predictions of diffusion-controlled models are also shown. Apparently, in both cases of Fig. 9, the diffusion-controlled model cannot describe the amplitudes and phases of the data, suggesting that a mixed kinetics model should be used, which is consistent with the inference from the constant-area adsorption experiments. Nonetheless, although the mixed kinetics model improves the fit in terms of the tension amplitudes and phase of the data, it too fails to match the data exactly. For the solution in buffer, comparisons of the diffusion-controlled model predictions and the data are shown in Fig. 10, and lead to the same conclusion as that from Fig. 9. The mixed kinetics model can improve the fits for most of the tension response curves, except for times close to those at $\gamma_{min}$ (the comparisons are not shown here). Indeed, in these cases the model predicts negative

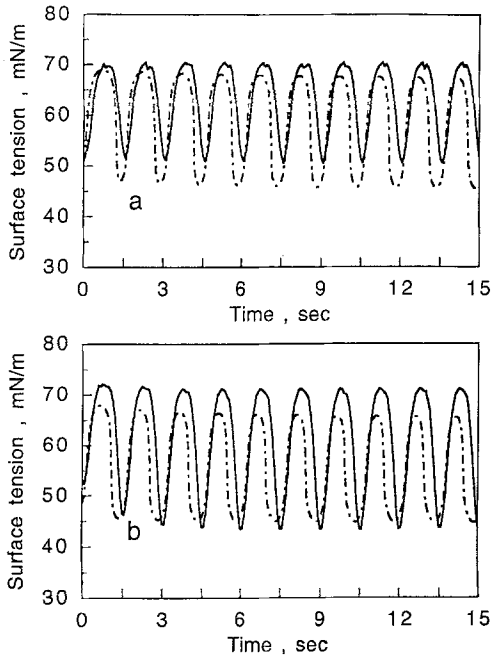


Fig. 10. Same as Fig. 9, but for solutions in phosphate buffer. Only predictions of the diffusion-controlled model are shown. Predictions of the mixed kientics model are poor; see text

$\gamma_{min}$ values, which are clearly due to $\Gamma/\Gamma_m$ (see Eq. (1)) being close to 1 or larger than 1. This is an artifact of the model used, in which the same surface equation of state is extended to any value of $\Gamma/\Gamma_m$. In reality, if the surface coverage $\Gamma$ is very close to $\Gamma_m$, the surface equation of state (Eq. (1)) ceases to be valid, inasmuch as the monolayer starts having significant repulsive interactions which can lead to monolayer collapse. This is analogous to the flat portion of the $\Pi$–A curves of insoluble monolayers near their collapse conditions. In more realistic models, one may use Eq. (1) up to a cutoff point of $\Gamma/\Gamma_m$, above which compressive stresses in the monolayer become overwhelming and lead to a limit in $\gamma_{min}$. Improved models may be reported in future communications.

## Conclusions

The equilibrium adsorption parameters $\Gamma_m$ and $K_L$ in the Langmuir isotherm for the surfactant DDAB · HCl in water and buffer solutions were estimated from the equilibrium adsorption behavior. A slightly larger value of $\Gamma_m$ for the buffer solutions suggests reduced electrostatic repulsions in the adsorbed monolayer. The larger value of $K_L$ obtained for the buffer solutions than for water suggests that the amphoteric form of the surfactant in buffer is more surface active than the cationic form in water solutions.

Dynamic tension behavior at constant-area conditions for this surfactant either in buffer or in pure water solutions show much longer adsorption timescales than the diffusion-controlled adsorption. The mixed kinetics adsorption model, which considers both diffusion and adsorption/desorption steps affecting the adsorption process, can fit the dynamic tension data well with appropriate $k_L^a$ and $B$ values, which vary with concentration [9]. The positive $B$ parameters are consistent with the existence of an activation energy barrier which may be caused by repulsive interactions between the surfactant molecules in the subsurface and the adsorbed monolayer.

The dynamic adsorption behavior for DDAB · HCl under pulsating-area conditions was also studied at different pulsating rates. The tension amplitude response $\Delta\gamma$ showed a strong dependence on concentration, first increasing with concentration and then decreasing. Although this behavior has been predicted before [10], it is reported here for the first time. The amplitude $\Delta\gamma$ depends also on frequency, usually increasing and sometimes reaching a plateau region for pulsating rates of about $\sim 90$ cycles · min$^{-1}$. The minimum surface tension $\gamma_{min}$ is always lower than the equilibrium surface tension, and decreases as the concentration increases for the water solutions. However, for the solutions in buffer it first decreases with the concentration and then increases.

Comparisons between the diffusion-controlled model predictions and the dynamic adsorption behavior under pulsating-area conditions support the conclusion that the adsorption process of DDAB · HCl is slower than predicted by the diffusion-controlled model. The mixed kinetics adsorption model provides better fits of the phase lag between area and tensions and the tension amplitude dependence on frequency, but it also needs improvements to describe the data quantitatively.

*Nomenclature*

| | |
|---|---|
| $B$ | empirical parameter in Eq. (3) |
| $c$ | concentration |
| $D$ | diffusivity |
| $k_L^a$ | adsorption rate constant |
| $k_L^d$ | desorption rate constant |
| $K_L$ | adsorption equilibrium constant |
| $n$ | factor accounting for the dissociation of counter-ions, Eq. (1). |
| $R$ | gas constant |
| $t$ | time |
| $T$ | temperature |

*Greek letters*

| | |
|---|---|
| $\gamma$ | surface tension |
| $\gamma_0$ | surface tension of pure solvent (water) |
| $\gamma_{min}$ | minimum surface tension |
| $\Delta\gamma$ | difference between maximum and minimum surface tensions |
| $\Gamma$ | surface concentration |
| $\Gamma_e$ | equilibrium surface concentration (subscript is dropped in Eq. (1)) |
| $\Gamma_m$ | maximum surface concentration |

*Acknowledgments*

This research was supported in part by the National Science Foundation (equipment grant #BCS91-1215Y), and by the Wool Foundation (U.K.) whose financial support to Dr. A. Pinazo allowed a six-month visit to Purdue University. We thank Dr. M.R. Infante for useful discussions.

**References**

1. Ernst R, Miller EJ Jr (1982) In: Bluestein BR, Hilton CL (eds) Amphoteric surfactants. Marcel Dekker, New York, pp 71–173
2. Idson B (1983) In: Rieger MM (ed) Surfactants in cosmetics. Marcel Dekker, New York, pp 1–28
3. Holzman S, Avram N (1986) Tenside Detergents 23:309–313
4. Wüstneck R, Kriwanek J, Herbst M, Wasow G, Haage K (1992) Colloids Surfaces 66:1–9
5. Hua XY, Rosen MJ (1988) J Colloid Interface Sci 124:652–659
6. Datyner A (1983) Surfactants in Textile Processing. Marcel Dekker, New York
7. Riva A, Cegarra J (1989) J Soc Dyers Colourists 105:399–405
8. Chang CH, Wang NHL, Franses EI (1992) Colloids Surfaces 62:321–332
9. Chang CH, Franses EI (1992) Colloids Surfaces 69:189–201
10. Chang CH, Franses EI (1993) Chem Eng Sci, in press
11. Rosen MJ, Zhao F, Murray S (1987) J Am Oil Chem Soc 64:439–331
12. Bregoff HM, Roberts E, Delwiche CC (1953) J Biol Chem 205:565–574
13. Lunkenheimer K, Miller R (1987) J Colloid Interface Sci 120:176–183
14. Lioussayre F, de Savignac A, Rico I, Hajjaji-Shriri N, Lattes A (1987) J Dispersion Sci Technology 8:181–197
15. Enhorning G (1977) J Appl Physiol: Respirat Environ Excercise Physiol 43:198–203
16. Rosen MJ (1989) Surfactants and Interfacial Phenomena. 2nd Edition. Wiley, New York
17. Steiner EC, Blau GE, Agin GL (1986) Introductory Guide: Simusolv Modeling and Simulation Software. The Dow Chemical Co., Midland, Michigan

Received March 22, 1993;
accepted May 3, 1993

Authors' address:

Professor E.I. Franses
School of Chemical Engineering
Purdue University
West Lafayette, IN 47907-1283,
USA